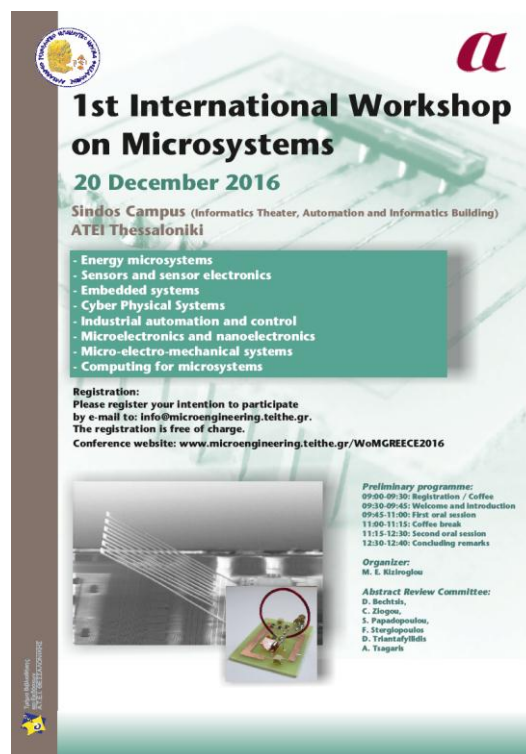




1st International Workshop on Microsystems

Sindos Campus, ATEI Thessaloniki, 20 December 2016



1st International Workshop on Microsystems

20 December 2016

Sindos Campus (Informatics Theater, Automation and Informatics Building)
ATEI Thessaloniki

- Energy microsystems
- Sensors and sensor electronics
- Embedded systems
- Cyber Physical Systems
- Industrial automation and control
- Microelectronics and nanoelectronics
- Micro-electro-mechanical systems
- Computing for microsystems

Registration:
Please register your intention to participate
by e-mail to: info@microengineering.teithe.gr.
The registration is free of charge.
Conference website: www.microengineering.teithe.gr/WoMGREECE2016

Preliminary programme:
09:00-09:30: Registrations / Coffee
09:30-09:45: Welcome and Introduction
09:45-11:00: First oral session
11:00-11:15: Coffee break
11:15-12:30: Second oral session
12:30-12:45: Concluding remarks

Organizer:
M. E. Kiziloglou

Abstract Review Committee:
D. Bechtak,
C. Zogou,
S. Papadopoulos,
F. Stergiopoulos,
D. Triantafyllidis,
A. Tsagaris

Workshop Proceedings

Introduction

This workshop brings together research and development from a large spectrum of science and engineering fields related to the implementation of microsystems in the new era of distributed information technologies. As cloud computing services and smart portable systems are becoming more widespread and more advanced, new possibilities for interdisciplinary research emerge. The microsystems that comprise the so-called internet of things will encompass a wide range of technological advancements including new energy sources, energy and information electronics, sensor systems, smart and energy efficient control and computing, telecommunications and networking, and also nanotechnology and micro-electro-mechanical systems. In this context, the 1st international workshop on Microsystems aims at bringing together related research and development advancements from the academic community and the industry. Scientific topics include but are not limited to:

Energy microsystems
Sensors and sensor electronics
Embedded systems
Cyber Physical Systems

Industrial automation and control
Microelectronics and nanoelectronics
Micro-electro-mechanical systems
Computing for microsystems

Michail E. Kiziroglou
m.kiziroglou@autom.teithe.gr

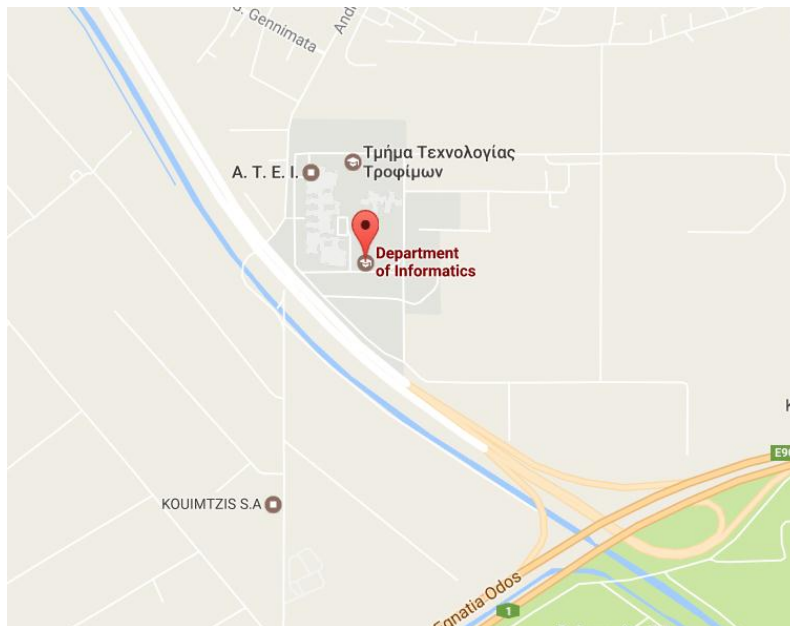
Venue

Informatics Theater

[Automation and Informatics Building](#)

Sindos Campus

ATEI Thessaloniki, Greece



Date

Tuesday, 20th of December, 2016

Reviewing Committee

Chrisovalantou Ziogou

Dimitrios Bechtsis

Simira Papadopoulou

Fotis Stergiopoulos

Dimitris Triantafyllidis

Apostolos Tsagaris

Organiser

Michail E. Kiziroglou

Registration Support

Themistoklis Koliass

List of Authors

No	Last Name	First Name	Affiliation
1	Bechtsis	Dimitris	ATEI Thessaloniki
2	Becker	Thomas	Airbus Group Innovations
3	Courson	R	LAAS-CNRS
4	Damigos	Alexios	ATEI Thessaloniki
5	Elefsiniotis	Alexandros	Airbus Group Innovations
6	Evans	James W.	UC Berkeley
7	Fouet	M.	LAAS-CNRS
8	Goodrich	Paython	LAAS-CNRS
9	Gue	A-M	LAAS-CNRS
10	Hahn	Sebastian	Airbus Group Innovations
11	Hatzikos	Evaggelos V.	ATEI Thessaloniki
12	Kalaitzakis	Konstantinos S.	ATEI Thessaloniki
13	Kalogianni	Eleni	ATEI Thessaloniki
14	Kamoutsis	Konstantinos	ATEI Thessaloniki
15	Kastopoulos	Alexandros	ATEI Thessaloniki
16	Kiziroglou	Michail E.	ATEI Thessaloniki
17	Menexes	Ioannis	ATEI Thessaloniki
18	Papadopoulou	Simira	ATEI Thessaloniki
19	Stergiopoulos	Fotis	ATEI Thessaloniki
20	Sylari	Antonios	ATEI Thessaloniki
21	Tastsidis	Vassilis	ATEI Thessaloniki
22	Triantafyllidis	Dimitris	ATEI Thessaloniki
23	Tselepis	Stefanos	ATEI Thessaloniki
24	Valeras	Andreas	ATEI Thessaloniki
25	Voutetakis	Spyros	CERTH
26	Wright	Steve W.	Imperial College London
27	Wright	Paul K.	UC Berkeley
28	Yeatman	Eric M.	Imperial College London
29	Yfoulis	Christos	ATEI Thessaloniki
30	Ziogou	Chrysovalantou	CERTH

List of Participating Organizations

Airbus Group Innovations, Germany

Alexander Technological Educational Institute of Thessaloniki, Greece

Centre for Research and Technology Hellas (CERTH), Greece

Imperial College London, U.K.

Laboratory for Analysis and Architecture of Systems (LAAS), CNRS, France

University of California at Berkeley, U.S.A.

Programme

09:00-09:30: Registration

Please pick up your badge or register at the front desk

09:30-09:45: Welcome and introduction

09:45-11:00: First Oral Session

09:45: Is One Pair Ethernet ready for take-off? *A. Elefsiniotis, S. Hahn (Invited, Airbus Group Innovations)*, 16WOM-01

10:15: Optimal Energy Distribution Strategy for a Fuel Cell Electric Vehicle. *A. Damigos, C. Ziogou, C. Yfoulis, S. Voutetakis and S. Papadopoulou*. 16WOM-02

10:30: Monitoring and control software tool for manufacturing processes, *I. Menexes, D. Bechtsis, F. Stergiopoulos and E. Kalogianni*, 16WOM-03

10:45: Hydrodynamic chip for blood microparticles sorting, *V. Tastsidis, M. Fouet, A-M Gué and R Courson*, 16WOM-04

11:00-11:15: Coffee Break and Poster Session

Power line energy harvester with a toroidal soft core loop, *A. Valeras and M. E. Kiziroglou*, 16WOM-05.

11:15-12:30: Second Oral Session (Session Chair: C. Ziogou)

11:15: Power Harmonics Considerations in Commercial Electronic Apparatuses, *A. Kastopoulos, D. Triantafyllidis and F. Stergiopoulos*, 16WOM-06.

11:30: A Custom Reflow Oven Controller Board, *S. Tselepis and M. Kiziroglou*, 16WOM-07.

11:45: Smart Home Automation using Arduino and Android, *A. Sylari, K. Stamatiou-Kalaitzakis, K. Kamoutsis, E. V. Hatzikos*, 16WOM-08.

12:00: Recent advancements in dynamic thermoelectric energy harvesting, *M. E. Kiziroglou, P. Goodrich, Th. Becker, S. W. Wright, E. M. Yeatman, J. W. Evans and P. K. Wright*, 16WOM-09.

12:15-12:30: Concluding remarks

WORKSHOP ABSTRACTS

Is One Pair Ethernet ready for take-off?

Alexandros Elefsiniotis, Sebastian Hahn

Airbus Group Innovations, Germany

Weight and cost are the two main driving factors for all novel vehicle technologies. Nowadays, as the need of information flow is increasing, higher data rates are required without increasing the two main factors. The automotive industry is gradually adopting Ethernet communication, while the railway and the aeronautical sector have been using Ethernet for a longer period, due to the high bandwidth that this technology offers. In aircraft more specifically, Ethernet has been used since the 1990s based on 10BASE-T. For newer aircraft control systems, like the current A380 and the A350, the avionics controllers are interconnected using 100BASE-TX. However, Fast Ethernet (100Mbps) requires two twisted pairs in order to achieve a bidirectional data link. A way to reduce weight, thus cost in this case, is to minimize the number of wires per cable by having new One Pair Ethernet standards (as the name implies one twisted pair cable with full duplex communication) like BroadR-Reach respectively 100BASE-T1 or newer standards like 1000BASE-T1. For Ethernet on copper, One Pair technologies are the first being designed for both harsh EMC environments and low cost availability as required by the automotive industry. Since EMC test procedures and limits are similar or even equal between automotive and aeronautic use cases, One Pair Ethernet is of high interest for future applications in aircraft. For this reason, in order to adopt BroadR-Reach technology (100BASE-T1) for future cabin applications, a study on coupling and protection circuits has been performed with different port configurations. Some of them are in combination with Power over Data Lines, the one pair equivalent to Power over Ethernet. Another advantage of this technology is that the automotive industry needs large quantities of One Pair Ethernet PHYs which will drive PHY prices down. This fact will enable different industries, i.e. aeronautical industry, to adopt the automotive components.



Optimal Energy Distribution Strategy for a Fuel Cell Electric Vehicle

A.Damigos⁽¹⁾, C. Ziogou⁽²⁾, C. Yfoulis⁽¹⁾, S. Voutetakis⁽²⁾, S. Papadopoulou⁽¹⁾

⁽¹⁾ Department of Automation Engineering, Alexander Technological Educational Institute of Thessaloniki, Thessaloniki, Greece

⁽²⁾ Chemical Process and Energy Resources Institute (CPERI), Centre for Research and Technology Hellas (CERTH), Thessaloniki, Greece

Abstract—The purpose of this work is to study energy management strategies for fuel cell electric vehicles, and implement an optimal control theory approach. The studied system is comprised of a Proton Exchange Membrane Fuel Cell (PEMFC), a Li-ion battery, a DC/DC converter and an electric motor fitted directly to the vehicle drive shaft. Using mathematical models for the components, an optimal energy distribution is computed for a given driving cycle.

I. INTRODUCTION

AS the concerns over climate change increase, alternative environmental friendly transport systems and renewable energy systems are becoming more attractive. In that context electric vehicles (EVs) and fuel cell EVs (FCEVs) aim to be part of the future transport sector [1]. Fuel cells are electrochemical devices that directly convert chemical energy stored in the fuel (in this case H₂) to electricity producing water and heat. Since there are no mechanical parts, they are very reliable (assuming the right operational conditions) and have a silent operation, a feature that together with the zero greenhouse emissions makes them very attractive for automotive use. Based on this motivation this work focuses on the optimal operation of an FCEV.

II. SYSTEM MODEL

In order to study the behavior of the FCEV, a model for each main subsystem (battery, fuel cell, motor, vehicle) is developed in MATLAB environment.

A. Li-Ion Battery

The battery model consists of a voltage source V_{src} in series with an internal resistance R_i . I_{batt} is the input, and V_{batt} the output. The state of charge is a state variable. Model equations [2]:

$$V_{batt} = V_{src} - R_i * I_{batt} \quad (1)$$

$$V_{src} = V_0 - K \frac{Q}{Q \int I_{batt} dt} + A \exp(-B \int I_{batt} dt) \quad (2)$$

$$K = \frac{(V_{full} - V_{nom} + A(\exp(-BQ_{nom}) - 1))(Q - Q_{nom})}{Q_{nom}} \quad (3)$$

$$Soc = 100 * \left(1 - \frac{\int I_{batt} dt}{Q}\right) \quad (4)$$

Where V_{full} is the fully charged voltage, V_{nom} is the nominal voltage, A is the voltage drop at the exponential zone, B is the charge at the end of the exp. zone, Q_{nom} is the nominal capacity and Q is the maximum capacity. To verify the validity of the battery model, its response was compared to typical operation of this subsystem according to data from the literature [1,2].

B. PEM Fuel cell

A semi-empirical model for the fuel cell is used [3]. Table 1 presents the input and output variable of the fuel cell model.

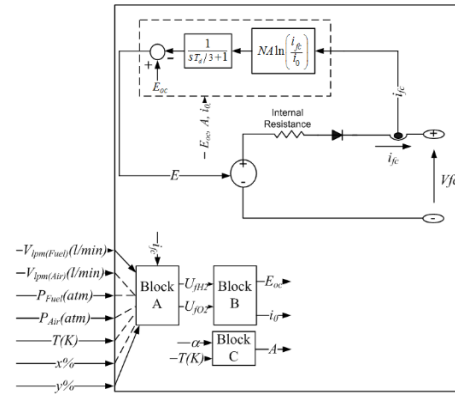


Fig.1 Fuel cell model overview

TABLE I
FUEL CELL MODEL SPECIFICATIONS

Inputs	Outputs
Air flow rate/pressure	Excess H ₂ (lamda)
Fuel flow rate/pressure	Excess O ₂ (lamda)
Percentage of H ₂ in the fuel mix	Voltage
Percentage of O ₂ in the air mix	
Operation Temperature	

The FC model response was validated in comparison to literature data as well.

C. Vehicle

The vehicle is modeled as a single point with three acting forces, the driving force coming from the motor, aerodynamic drag and friction. Using Newton's law, we can compute the acceleration and thus the speed and position of the vehicle on one axis. The input is the torque at the motor shaft and the outputs are the motor shaft angular velocity, the vehicle speed and acceleration and the traveled distance.

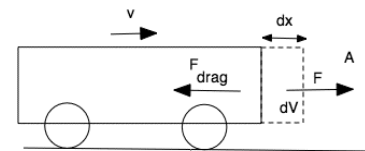


Fig.2 Vehicle model diagram

$$\text{VehicleSpeed} = \int \text{Acceleration} dt \quad (5)$$

$$\text{Acceleration} = \frac{\Sigma F}{m} = \frac{F_{\text{mot}} - F_{\text{drag}} - F_{\text{roll}}}{m} \quad (6)$$

$$F_{\text{mot}} = \frac{\tau}{r}, F_{\text{drag}} = 0.5\rho AC_d u^2 \quad (7)$$

$$F_{\text{roll}} = (C_0 + C_1|u| + C_2u^2)mg \quad (8)$$

Where:

m: vehicle mass (kg), τ : motor torque (Nm), r: wheel radius (m), n: gear ratio, ρ : air density (kg m^{-3}), g: gravity (m s^{-2}), A: vehicle frontal area (m^2), C_n : coefficients, F_{mot} : force induced by the motor (N), F_{drag} : force of the aerodynamic drag (N), F_{roll} : rolling resistance force (N).

III. OPTIMAL OPERATION

At each simulation step, the required torque (T_{sp}) is computed using the driver input (pedal) and the current motor speed. The fuel cell and battery currents are provided by the optimizer, so using the models we can determine the power drawn from each (or the charging power, in case of regenerative braking). Thus, using the current motor speed we can determine the torque that will be produced by the motor, which is then inputted to the vehicle model. By combining multiple (weighted) targets on our cost function we can optimize different aspects of the system. A Non-Linear Programming (NLP) formulation is applied using a Sequential Quadratic Programming (SQP) method. The cost function is analyzed at Eq. 9:

$$J = w_1(T_{sp} - T) + w_2\left(1 + \frac{I_{\text{batt}}}{|I_{\text{batt}}|}(1 - e^{-|I_{\text{batt}}|}) \frac{\text{Soc}_d - \text{SOC}}{\text{Soc}_d - \text{Soc}_{\text{min}}}\right) \quad (9)$$

The optimizer tries to minimize the cost function by adjusting I_{batt} and I_{fc} . The value of the currents determines the power that is available to the motor, which is translated to torque. The first term ($T_{sp} - T$) means that the optimizer will provide enough power to match the torque requirements of the user. The second term is a sigmoid function which increases proportionally to 1) the difference of the current SOC value from the desired, 2) the battery current. As such, the battery tends to stay at the desired SOC and it is used only when the fuel cell cannot meet the power demands. A battery that is never fully charged makes sure that any power generated from braking will always be absorbed. The weights (w_1, w_2) are the tuning parameters which determine how much impact each term has. Increasing w_1 for example means that more attention is given on the effort of matching the requested torque.

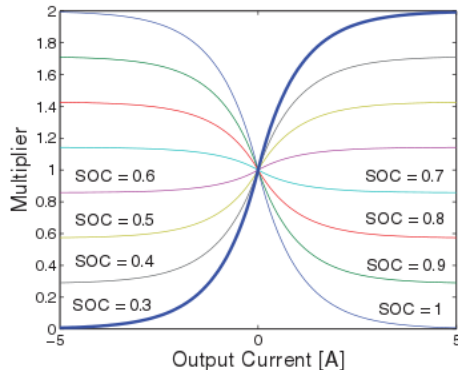


Fig.3 Cost function sigmoid term

TABLE II

OPTIMIZATION CONSTRAINTS

Fuel cell	Battery	MOTOR
$I_{\text{fcmin}} = 0 \text{ A}$	$I_{\text{battmin}} = -4 \text{ A}$ (0.2C charge)	$T_{\text{max}} = 256 \text{ Nm}$
$I_{\text{fcmax}} = 347 \text{ A}$	$I_{\text{battmax}} = 80 \text{ A}$ (4C)	

IV. RESULTS ANALYSIS OF THE OPERATION

In order to evaluate the response of the proposed optimization-based energy distribution strategy a simulation for 500s with 1s step, 5s optimization step and $P_{\text{fc,lim}} = 50\text{kW}$ was performed.

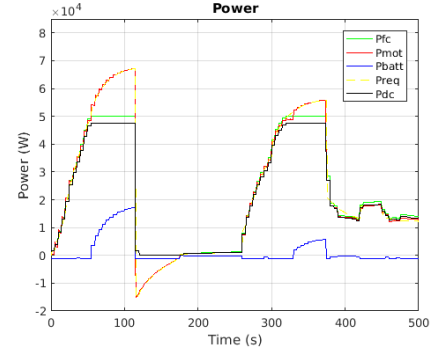


Fig.4 Power Distribution

(fuel cell, motor, battery, requested and DC/DC converter)

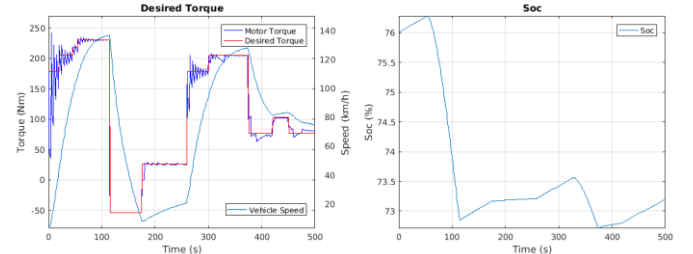


Fig.5 a) Torque and Speed b) Battery State of Charge

It is concluded from the Figs 4 and 5 that the optimization-based energy distribution strategy can fulfill the user's torque demands (albeit with some oscillation). Also the strategy is considering the long-term effects of the battery depletion and as such utilizing it only when the fuel cell can't provide sufficient power.

V. FUTURE WORK

As future work, a set of additional controlled and manipulated variables will be added to the system, such as manipulating hydrogen and air flows in order to control their excess ratio (λ). The development of a model predictive approach for the control of the integrated system is in progress.

REFERENCES

- [1] D. Dörffel, "Peace-of-Mind Series Hybrid Electric Vehicle Drivetrain: Transfer Thesis (MPhil/PhD)," 2003.
- [2] O. Tremblay and L.-A. Dessaint, "Experimental validation of a battery dynamic model for EV applications," World Electr. Veh. J., vol. 3, no. 1, pp. 1–10, 2009.
- [3] O. Tremblay, L.-A. Dessaint, and others, "A generic fuel cell model for the simulation of fuel cell vehicles," in 2009 IEEE Vehicle Power and Propulsion Conference, 2009, pp. 1722–1729.

Monitoring and control software tool for manufacturing processes

Ioannis Menexes¹, Dimitrios Bechtsis¹, Fotis Stergiopoulos¹, Eleni Kalogianni²

1 Department of Automation Engineering, Alexander Technological Educational Institute of Thessaloniki

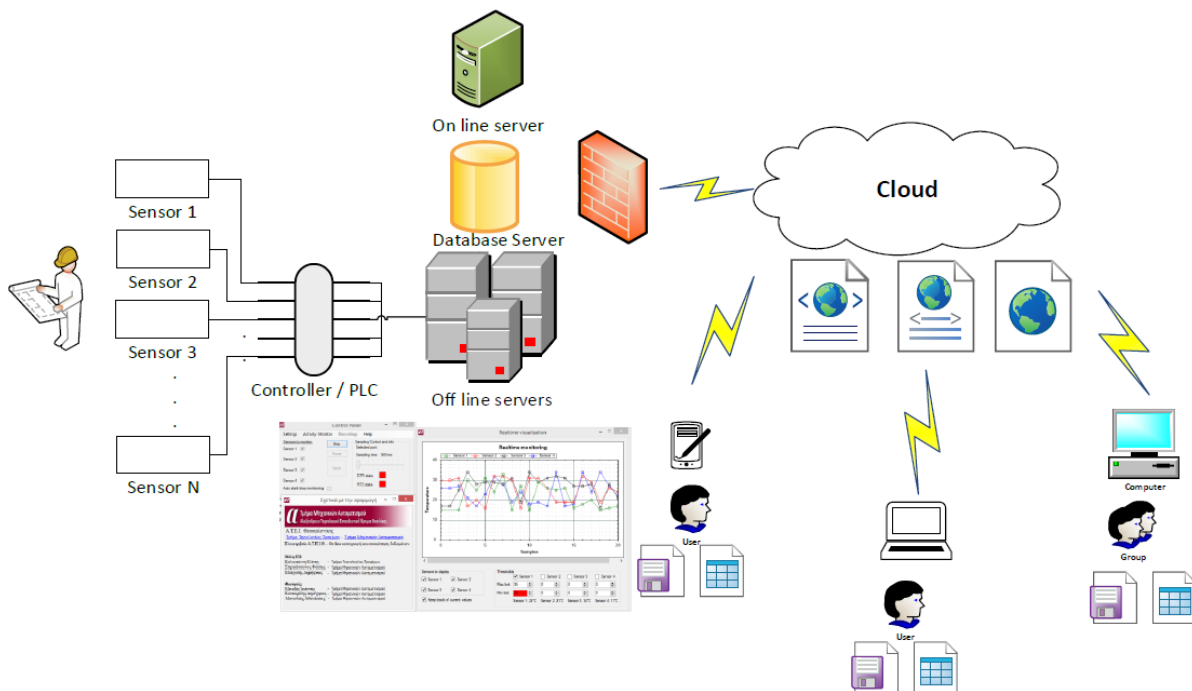
2 Department of Food Technology, Alexander Technological Educational Institute of Thessaloniki

Monitoring of manufacturing processes can provide significant advances in equipment life and product quality and furthermore improve visibility and trackability in the digital supply chain context. On the other hand automation and control are of major importance for flexible and sustainable manufacturing systems that minimize labor costs, reduce down time and operation and maintenance (O&M) costs. In this context an efficient Monitoring and Control software Tool (MCT) for manufacturing systems is proposed. The overall system architecture includes four discrete levels: (a) Embedded sensors in the production line for data gathering, (b) Data aggregation at a microcontroller or a Programmable Logic Controller (PLC), (c) Data management at the of-line server, and finally (d) On-line data monitoring from a web based interface.

Embedded production sensors provide raw data to the microcontroller with the use of external hardware interfaces. The microcontroller handles raw data by using specific sampling rates and finally supports bidirectional wireless or wired data communication with the mainframe computer. The MCT recognizes the available sensors for each recording, schedules recordings at specific sampling rates, provides data visualization screens for all sensors (real-time and historical values of the sensor), identifies out of range values and provides appropriate feedback to the system and the user and finally saves the recording in the popular XML (eXtensible Markup Language) format. Moreover the proposed tool can compare specific sensors from historical data and export historical recordings to the popular CSV (Comma Separated Values) format for promoting interoperability with third party software. The tool is developed in the C# programming language.

The proposed system architecture is to be tested in a real-world application that includes a small-industrial scale olive oil producing facility located at A.T.E.I.Th. Further work will examine the use of data and their incorporation into process design procedures as well as the existence of a web based interface for real-time monitoring of manufacturing processes.

Acknowledgements: The development of the pilot system is part of several on-going projects supervised by the Department of Automation Engineering and the Department of Food Technology of the Alexander Technological Educational Institute of Thessaloniki (A.T.E.I.Th.). We would like to thank the undergraduate students of the Department of Automation Engineering Mr. Dimitrios Katikaridis, Mr. Giorgos Kontovos, Mr. Athanasios Manolios, Mr. Ioannis Menexes and Mr. Pavlos Savlaras for their contribution to the ongoing development process.



Hydrodynamic chip for blood microparticles sorting

V Tastsidis¹, M Fouet², A-M Gué², R Courson²

¹ATEI Thessaloniki, Greece

²LAAS Toulouse, France

The passive, filter-less method is able to sort microparticles from a complex sample using the hydrodynamic effects in microchannels. The principal concept of the microfluid device is based on the velocity profile and the hydrodynamic resistance which are capable to obtain the device properties in order to reach the desirable particles, by sorting them according to their size. The design and the fabrication of the microfluid device applied on the 3D architecture model based on a lamination technique. The fabrication and characterization process corresponds to a sweep from 300 μm to 5 μm for the lateral channel dimensions. This is suitable for sorting microparticles down to 0.5 μm . Adapting another methodology and modifying the device from single lateral channel up to N-channels, is demonstrated. This can increase the efficiency on flow rate/volume and time/volume. The characterization process indicates clogging issues in most of the lateral channels, imputing complication during the fabrication and developing of the device. Despite this collision, results confirmed the principle and the isolating ability of the chip, which provides prospects on continuing the research. Blood microparticles sorting devices have a special interest in medical and biological domains: hematology, cancerology, biotechnology. Applications of isolating and characterize particles such as monitoring tumor cells, provide new aspects for numerous therapies and health issues.

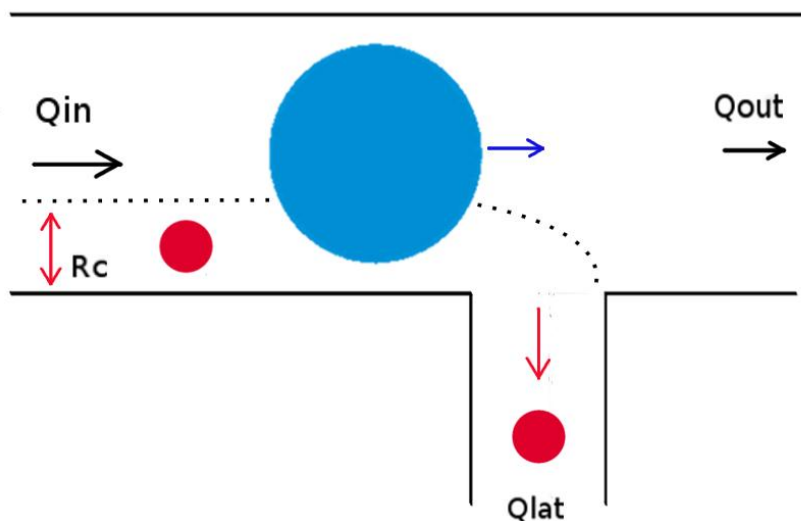


Figure 1: The main principle for the microparticles sorting devices

Power line energy harvester with a toroidal soft core loop

A. Valeras and M. E. Kiziroglou

ATEI Thessaloniki, Greece

Harvesting energy from low voltage grid power lines may be useful for permanently installed line monitoring systems. Relevant sensing application may include power metering but also temperature and other environmental conditions in industrial networks. A non-invasive energy harvesting approach offers installation simplicity and overcomes requirements for additional powering transformer and measuring circuitry which imply additional costs and reduced overall system reliability. In comparison with battery based systems, this approach offers a significant advantage with regard to maintenance overheads that are introduced when battery replacement or recharging is required. Power line energy harvesting prototypes using magnetic MEMS structures and other methods have been previously reported [1]. In addition, powering aircraft wireless sensors by inductive harvesting from variable-frequency aircraft power lines has been demonstrated [2]. In this work, we present a simple inductive harvesting prototype, based on a commercial toroidal soft core transformer. A simple power measuring circuit is used to characterize the device performance for different power line current values, in the current range and frequency of typical low-power electrical installations. The maximum power transfer point using an ohmic load is identified. Harvested power of 50 mW, 26 mW and 6.6 mW are demonstrated from 220 V, 50 Hz power lines at 5.5 A, 3.6 A and 1.8 A respectively as shown in Figure 1. These results demonstrate the viability of power line harvesting as a method for delivering power to low electrical power networks.

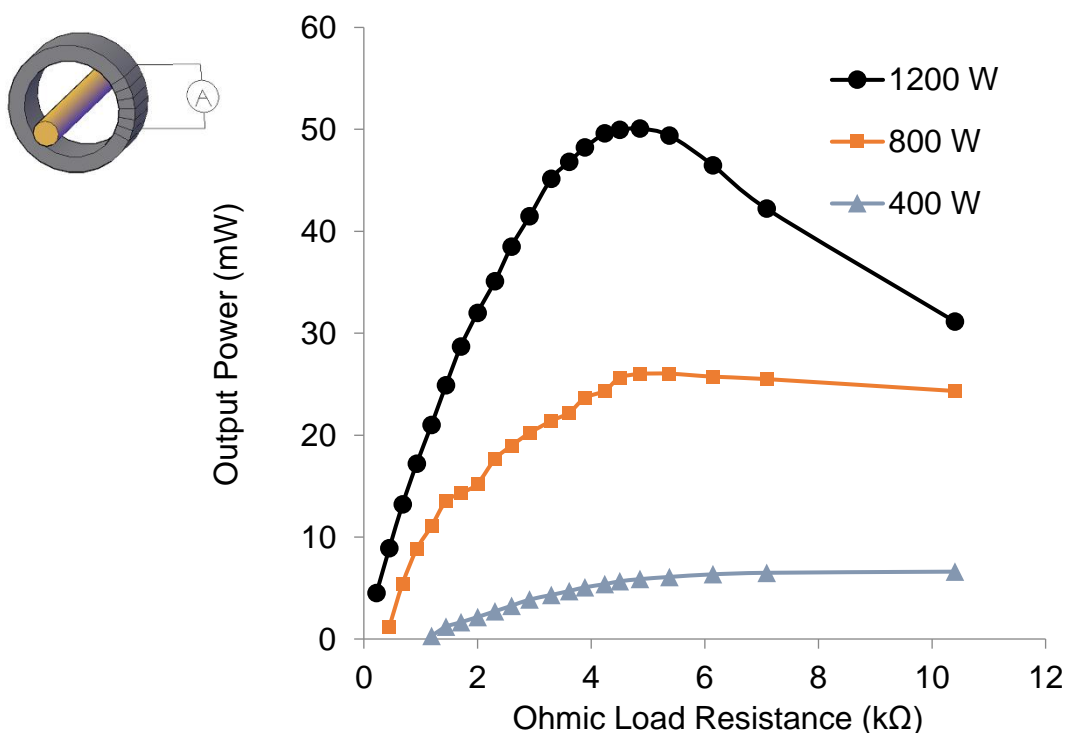


Figure 1: Experimental results of power harvested from a 220 V, 50 Hz power line using a commercial toroidal ring transformer.

References

- [1] Leland et al, "Energy scavenging power sources for household electrical monitoring," in Proceedings of the 6th Int. Workshop on Micro and Nanotechnology, pp. 165–168, Berkeley, Calif, USA, 2006
- [2] Toh et al, Inductive energy harvesting from variable frequency and amplitude aircraft power lines, Nov. 18–21, PowerMEMS, Hyogo, Japan, 2014, J. Phys.: Conference Series 557 (2014) 012095

Power Harmonics Considerations in Commercial Electronic Apparatus

A. Kastopoulos*, F. Stergiopoulos* and D. Triantafyllidis*

* Alexander Technological Educational Institute of Thessaloniki / Department of Automation Engineering,
P.O. Box 141, 57 400 Sindos, Thessaloniki, Greece
alexakoss18@hotmail.com, fstergio@autom.teithe.gr, drdimitri@autom.teithe.gr

Abstract — The present paper discusses the important issue of power harmonics at the load side in commercial electronic equipment. Examples of harmonic spectrums and basic definitions are presented. Furthermore, simulation results and their comparison with experimental results are presented for a simple electronic circuit built for this purpose, as well as experimental results taken from a commercially available Uninterruptible Power Supply.

I. INTRODUCTION

Major technological advancements in the last decades have resulted in a quite significant use of electronic devices and apparatus in peoples' everyday lives and activities. These pieces of equipment have been designed so as to support our work, as well as personal and leisure activities. This fact has also resulted in a corresponding tremendous increase of power electronics-based converters and systems that have the role of providing power to the equipment by means of converting the available AC mains 230V, 50Hz voltage to appropriate AC and DC voltages of suitable magnitude.

As known, electronic power conversion is based on the use of switching semiconductor devices such as power Diodes, MOSFETs, JFETs, IGBTs, etc. Based on the switching pattern of such devices, suitable waveforms are then produced which power the electronic apparatus. This switching action, however, results in the rise of power harmonics which impose a number of significant detrimental effects such as the reduction of power factor, the increase of cable losses, increased cable voltage and current ratings, occurrence of resonances, etc. As a result, the issue of electrical power quality has emerged. This issue has been studied extensively regarding large industrial users, but less attention has been paid to users of commercial (domestic) devices of relatively small power levels. As the issue of power quality is directly related to energy efficiency and rational use of energy, it is mandatory to proceed to studies and demonstration of related issues in commercial electronic apparatus, in order to provide a means of informative presentation and discussion among users [1-10].

The paper is organized as follows: In Section II an example of a commercially available electronic apparatus, highly popular, such as an Uninterruptible Power Supply (UPS), and its load side harmonics is presented and basic measured variables are introduced. In Section III a more detailed analysis of a simple electronic circuit built as a demonstrator for a light dimming application is given, supported by both simulation and experimental results

concerning power harmonics. Finally, Section IV concludes the paper.

II. AN ILLUSTRATIVE EXAMPLE: A UPS DEVICE

Uninterruptible Power Supplies (UPS) are quite common and popular electronic apparatus used in various applications to provide alternative means of power supply in the case of a grid failure. Most commonly, these devices are used by the general public to provide power to Personal Computers (PCs), the aim being to avoid loss of data in the case of a sudden and unexpected power outage. For example, Figure 1 presents an indicative specimen, rated at 500W:



Figure 1. An indicative specimen of a commercially available UPS device

The principle of operation of a UPS device is quite straightforward: during normal operation, the load of the device (e.g. a PC) is powered by the grid which also charges a battery (usually of a lead acid type). In the case of a grid failure, power is supplied to the load by the battery via an electronic DC/AC converter (inverter).

However, one should note that the resulting AC load voltage waveform in the case of a grid failure is not always sinusoidal. Most UPS types operate their inverter in a simple manner, producing a symmetrical waveform with a dual polarity, e.g. a trapezoidal signal. This type of operation is characterized by simplicity (and thus lower cost) in its implementation and even though it may not produce significant problems in certain types of loads, quality issues may rise in the case of sensitive electronic loads for which the particular UPS is improper. This is mainly due to the fact that non-sinusoidal waveforms give rise to power harmonics of usually low order that, in many cases, can affect the operation of the load of the UPS.

For example, Figure 2 presents the load voltage of the UPS device presented in Figure 1, as recorded using a FLUKE 41B Power Harmonics Analyzer, during normal operation, i.e. power delivered through the grid.

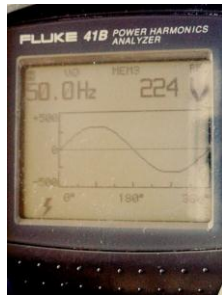


Figure 2. Load side voltage of the UPS device presented in Figure 1 under grid supply mode

However, in the case of a grid failure (e.g. power outage), the load is supplied from the battery through a DC/AC inverter, producing a trapezoidal waveform, as shown in Figure 3:

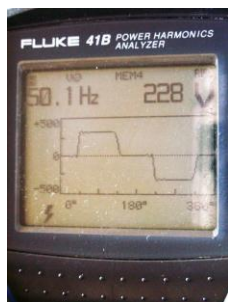


Figure 3. Load voltage during a power outage

The waveform in Figure 3 gives rise to a series of low order odd harmonics (e.g. 3rd, 5th, 7th, etc), resulting to a deterioration of the power quality of the load voltage. Figure 4, presents the measured harmonic spectrum of the voltage waveform of Figure 3, where clearly a number of low order harmonics of significant magnitude is measured.

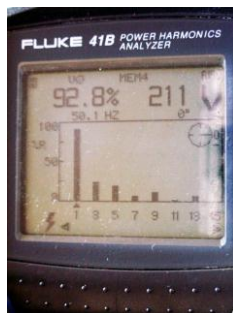


Figure 4. Load side power harmonics

A very common index directly associated with power quality is the Total Harmonic Distortion (THD), which associates the values of the magnitudes of the harmonics with respect to the fundamental frequency of 50 Hz. The index, e.g. in the case of load voltage is defined as follows:

$$THD = \frac{\sqrt{\sum_{h \neq 1}^{\infty} V_h^2}}{V_1} \quad (1)$$

Where V_h is the peak or rms value of the voltage harmonic of order h and V_1 is the peak or rms value corresponding to the fundamental frequency. Ideally, i.e. in

the case of purely sinusoidal (50Hz) waveforms, this index is equal to zero. As seen in Equation (1), this index sums up the results of all harmonics and compares it to the fundamental. The measured THD value of the waveform presented in Figure 3 was 40.2%.

As a result of the presence of power harmonics, the load voltage is increased. For example, assuming that rms values are used in Equation (1), the resulting rms value of the load voltage is given by:

$$V_{rms} = V_1 \sqrt{1 + (THD)^2} \quad (2)$$

Furthermore, the presence of voltages with frequencies other than the fundamental frequency of 50Hz, gives rise to current harmonics, producing power losses that reduce the efficiency of the equipment. In addition, the presence of harmonic power, results in a reduction of the power factor of the device, as seen from the grid side [11-14].

Therefore, one should always be careful about the selection of a UPS device for a particular application, as the presence of harmonics may affect the quality of operation of the equipment as well as reduce its efficiency. [15-17].

III. THE CASE OF A SIMPLE LIGHT DIMMER APPLICATION

In order to consider the issue of load side power harmonics further, a simple electronic circuit that can be used for light dimming applications has been built. Figure 5 presents a photograph of the circuit built in the Laboratory of Power Electronics of the Department of Automation Engineering, whereas Figure 6 presents its basic circuit schematic. As seen in Figure 6, the basic element of the circuit is a power MOSFET switch. Light dimming is derived by altering the firing angle α of the switch within a range between $\alpha=0^\circ$ (full light intensity) and $\alpha=180^\circ$ (minimum light intensity).



Figure 5. Simple electronic circuit built for light dimming applications

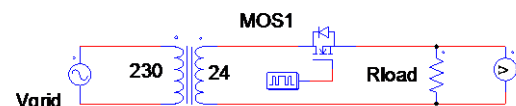


Figure 6. Circuit schematic

For the purpose of producing results for various cases, three values of the firing angle α have been selected, namely $\alpha=36^\circ$, $\alpha=76^\circ$ and $\alpha=136^\circ$. For example, Figure 7 presents the measured waveform of the load voltage (across the terminals of the light bulbs in Figure 5) for the case of $\alpha=76^\circ$:

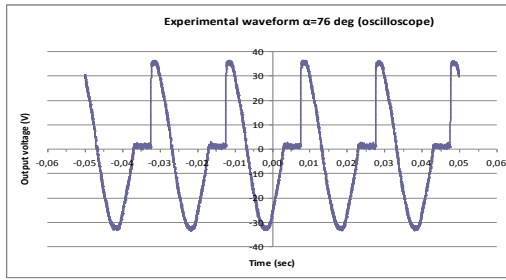


Figure 7. Measured waveform of the load voltage in the case of $\alpha=76^\circ$

The effect of the firing angle is clearly seen in Figure 7, affecting the conduction interval of the switch, thus altering the rms value of the resulting waveform, adjusting the intensity of the light.

As an effect of the switching action of the power device (MOSFET) switch, voltage harmonics are produced. Figure 8, presents the measured harmonic spectrum of the waveform of Figure 7, using a Digital Oscilloscope with integrated Fast Fourier Transform (FFT) analysis.

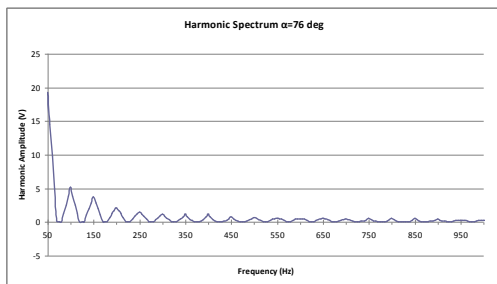


Figure 8. Harmonic spectrum of the load voltage in the case of $\alpha=76^\circ$

The magnitudes of the most significant harmonics, up to the 14th order (corresponding to a harmonic frequency of 700Hz) have been recorded for each of the three cases of the firing angle α . Then, the approximate THD index was calculated, based on Equation (1), as:

$$THD \approx \frac{\sqrt{\sum_{h=1}^{14} V_h^2}}{V_1} \quad (3)$$

where the lower script (1) corresponds to the fundamental frequency of 50Hz. The results of the measured THD indices are given in Table I and are presented graphically in Figure 9. As seen in Figure 9, an almost linear relationship is recorded and exists between the firing angle and the resulting THD index.

TABLE I. CALCULATED THD INDEX USING MEASUREMENTS

Firing angle α (degrees)	THD (%)
36	14,79
76	42,16
136	89,36

As can be seen in Table I and Figure 9, serious concerns about power quality are raised in the case of large values of the firing angle α which (physically) correspond to reduced light intensity. Therefore, for these values one should expect

an exaggeration of issues related to a significance presence of power harmonics.

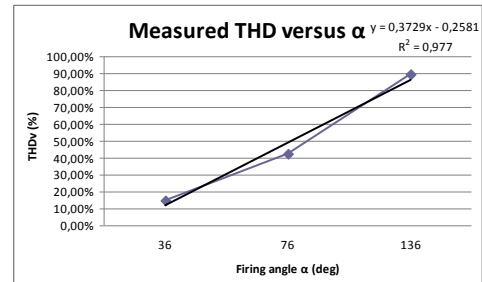


Figure 9. Graphical representation of the data of Table I

The results derived experimentally were also compared to simulation results derived using the PSIM[®] software programme. For example, Figure 10 presents the simulated waveform of the output voltage in the case of $\alpha=76^\circ$, which is in quite good agreement with the measured waveform presented in Figure 7:

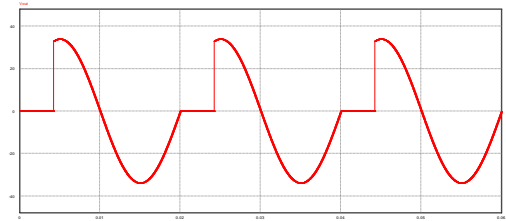


Figure 10. Simulated waveform of the load voltage in the case of $\alpha=76^\circ$

THD index values have also been calculated in simulation. The results are presented in Table II, and are in quite good agreement with the measured values presented in Figure 1:

TABLE II. CALCULATED THD INDEX IN SIMULATION

Firing angle α (degrees)	THD (%)
36	14,82
76	41,54
136	89,83

IV. CONCLUSIONS

In the previous Sections, considerations regarding load side power harmonics were presented and discussed for commercial electronic equipment. In order to facilitate the discussion two indicative examples were presented including a commercially available UPS device and an electronic circuit built in the Laboratory for simple light dimming applications. As shown, both in experiment and simulation, harmonic frequencies of significant magnitudes arise producing a number of detrimental effects regarding mainly power losses, deterioration of the power factor, increased stresses etc. Further work will theoretically model the harmonics produced and provide analytical results regarding the electrical characteristics of various circuits employing power electronic switches [18].

The results can be used as a demonstration example in the educational process of the Department of Automation Engineering and offer a handle for further investigation in the field of power quality of power electronic converters.

Furthermore, the analysis presented could be generalized and could be used in an equipment characterization process assessing the effects of harmonics on energy efficiency and the level of rational use of energy in several popular types of electronic apparatus [19].

REFERENCES

- [1] H.E. Mazin, W. Xu, and B. Huang, "Determining the harmonic impacts of multiple harmonic-producing loads," *IEEE Trans. Power Delivery*, vol. 26, no. 2, pp. 1187–1195, April 2011.
- [2] C. Jiang, D. Salles, W. Xu, and W. Freitas, "Assessing the collective harmonic impact of modern residential loads—part II: applications," *IEEE Trans. Power Delivery*, vol. 27, no. 4, pp. 1947–1955, Oct. 2012.
- [3] M.-Y. Chan, K. KF Lee, and M. WK Fung, "A Case Study Survey of Harmonic Currents Generated from a Computer Centre in an Office Building," *Architectural Science Review*, vol. 50, no. 3, pp. 274–280, Sep. 2007.
- [4] V. Bećirović, B. Nikolić, S. Hanjalić, M. Brkić, "Modeling a Group of Consumers in Order to Analyze Power Quality," 4th International Youth Conference on Energy, 6-8 June 2013, publ. IEEE.
- [5] S. Puchalapalli and N. M. Pindoriya, "Harmonics Assessment for Modern Domestic and Commercial Loads: A Survey," *International Conference on Emerging Trends in Electrical, Electronics and Sustainable Energy Systems*, 11-12 March 2016, publ. IEEE."
- [6] C. J. Gajanayake, G. Ramtharan, G.K. Samaraweera, A. Atputharajah, J.B. Ekanayake, "A survey of harmonic currents at several industries in Sri Lanka," *J. Natn Sci. Foundation Sri Lanka*, vol. 33, no 3, pp. 205–217, 2005.
- [7] H. Farooq, C. Zhou, M. E. Farrag, "Analyzing the Harmonic Distortion in a Distribution System Caused by the Non-Linear Residential Loads," *Int. J. of Smart Grid and Clean Energy*, vol. 2, no 1, January 2013.
- [8] S. Saha, S. Das, C. Nandi, "Harmonics Analysis of Power Electronics Loads," *Int. J. Comp. Applications*, pp. 32-36, vol. 92, no.10, April 2014.
- [9] K. N. Sarpong, K. Sarfo, J. F. Rushman, A. Donkor, "Load Assessment/Evaluation of a Three Phase Four Wire Distribution System of a Technical Institution. A Case Study of Kumasi Polytechnic, Ghana," *Int. J. Science and Research*, pp. 147-153, vol. 5, no. 6, June 2016
- [10] S. T. Elphick, S. Perera and P. Ciufu, "Supply current characteristics of modern domestic loads," *AUPEC 2009*, pp. 1-6. 2009.
- [11] N. Locci, C. Muscas, and S. Sulis, "Detrimental effects of capacitors in distribution networks in the presence of harmonic pollution," *IEEE Trans. Power Delivery*, vol. 22, no. 1, pp. 311–315, Jan. 2007.
- [12] Francisco C. De La Rosa, "Harmonics and power systems," *CRC/Taylor & Francis: Boca Raton*, 2006.
- [13] J. Arrillaga and N. R. Watson, "Power System Harmonics," 2nd ed., *J. Wiley & Sons: England*, 2003.
- [14] A. Harrison, "The Effects of Harmonics on Power Quality and Energy Efficiency," *Dissertation, Dublin Institute of Technology* 2010.
- [15] *IEEE Recommended Practice and Requirements for Harmonic Control in Electric Power Systems*, IEEE Std 519-2014 (Revision of IEEE Std 519-1992), pp.1-29, June 11 2014.
- [16] IEC 61000-3-2, "Electromagnetic compatibility (EMC) –Part 3-2: Limits – Limits for harmonic current emissions (equipment input current ≤ 16 A per phase)," Bureau Central de la CEI, 3 rue de Varembe, CH-1211, Geneva 20, Suisse.
- [17] Jens Schoene, "Evaluation of the Impact on Non-Linear Power On Wiring Requirements for Commercial Buildings, Final Report," *The Fire Protection Research Foundation, One Batterymarch Park, Quincy, MA, USA*
- [18] A. Zoha, A. Gluhak, M. A. Imran and S. Rajasegarar, "Non-Intrusive Load Monitoring Approaches for Disaggregated Energy Sensing: A Survey," *Sensors*, vol. 2012, no. 12, pp.16838-16866, 2012.
- [19] C. Calwell, T. Reeder and N. Horowitz, "Power Supplies: A Hidden Opportunity for Energy Savings," *Natural Resources Defense Council*, May 2002.

A Custom Reflow Oven Controller Board

S. Tselepis and M. E. Kiziroglou

Department of automation engineering, ATEI Thessaloniki
developer.fire@gmail.com

I. INTRODUCTION

In this work, a methodology for converting a normal convection oven to an oven capable to follow thermal profiles with accuracy suitable for reflowing Prototype Circuit Boards is proposed [1-4]. The proposed system includes an integrated human-machine interface (HMI) system with touch screen LCD and supports further monitoring from a computer. The profiles generation is also integrated to the same computer program which also includes some other extra minor features.

Major PCB manufacturing companies such as LPKF [5] and BUNGARD [6] offer industrial grade reflow ovens. However, commercial models are often expensive and not customized to the requirements of specific project requirements. The objective of the system proposed here is to achieve a home-made implementation that is affordable to education level projects, while maintaining an industrial level reflow quality. In addition, an open-source policy for both software and hardware is adopted, in order to achieve a universally applicable and configurable fabrication methodology.

The controller has a very simple job, to follow a profile curve defined by the profile data. It does that with the help of a PID controller, integrated into the microprocessor. A typical challenge in such a case is that if the controller has static gains, the overshoot becomes very high, when a fast temperature transition is required.

To solve this problem, a profile generator was developed, where the user draws the desired profile line by placing points with individually and dynamically configurable PID gains. An example profile as displayed by the system software is shown in Figure 1. The standard instruction set between software and microcontroller makes possible to use a typical SCADA application for controlling and monitoring the system. Profile design may be impossible or extremely complicated to implement in a typical SCADA application.

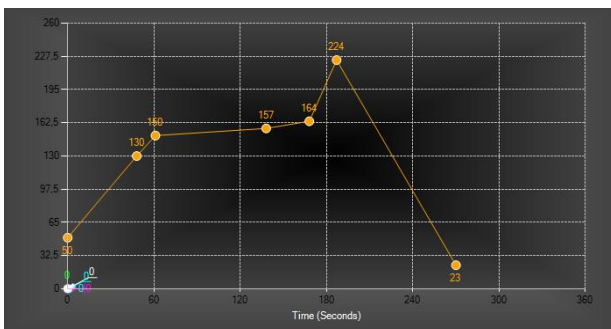


Figure 1. A simple reflow profile defined with points of configurable PID parameters.

II. HARDWARE

The heart of the controller is an ATMEGA2560 microcontroller [7]. For the temperature monitoring, there are two MAX31855 Cold Junction Compensated Thermocouple to Digital Converters [8]. For data storage, the controller is connected to a MicroSD card. In addition, there is a Real-Time-Clock based on the DS3231. For the HMI system, an NEXTION TFT-LCD module with intergraded microcontroller for graphics rendering is employed. Data transfer between PC and controller is made by a galvanically isolated FT232 UART to USB Converter [9-11].

This custom microcontroller module system comprises plenty of outputs. It includes four SPDT dry contacts Relays and three PWM outputs, which are configurable both from the microcontroller LCD and the PC. In this way, the user is able to connect more heating elements, fan, indicators, etc. Every pin on ATMEGA is connected with a socket and a long pin header so that the user can use any pin to connect an external upgrade board such as an Ethernet or a Bluetooth module.

PWM is in Phase and Frequency correct mode and its purpose is to switch the heating elements by driving external Solid States relays. It works on a constant period on 1sec equally to sample time. Solid states relays have galvanic isolation, they switch on crossover which doesn't generate noise and they don't have mechanical contacts to wear out from constant switching. On board relays are designed to drive any external low current implementation threw isolated dry contacts.

A first implementation using an in-house PCB fabrication facility is shown in Figure 2. After successful functional testing at this level, the system was designed in the Altium Designer computer simulation software (Figure 3), and fabricated using a general purpose commercial PCB fabrication service. The fabricated PCB is presented in Figure 4.

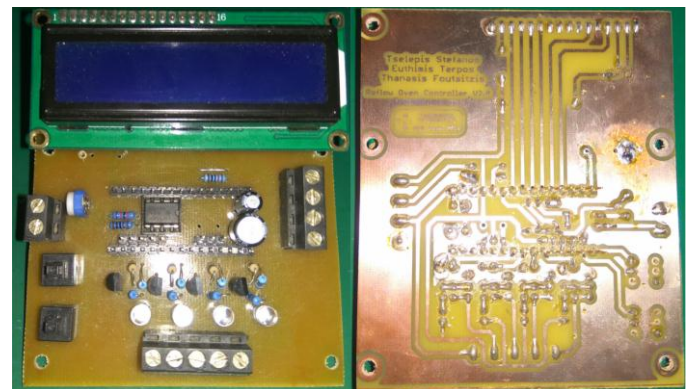


Figure 2. In-house made first prototype PCB.

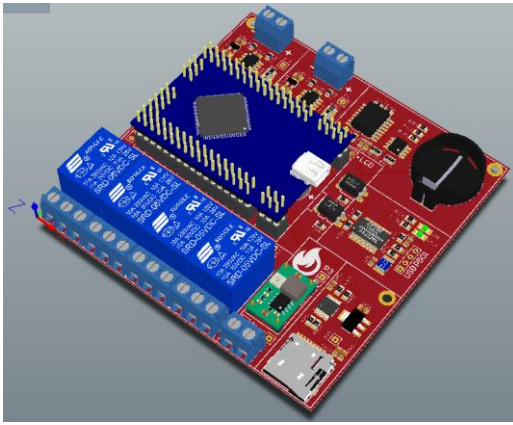


Figure 3. Altium Designer 3D Model of the board.

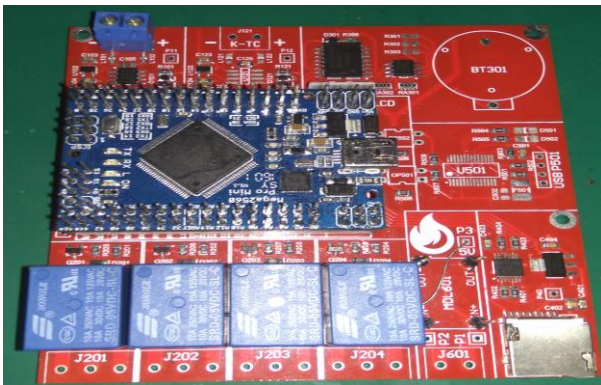


Figure 4. Latest version of the controller PCB manufactured by an external PCB service.

III. SOFTWARE DEVELOPMENT

For software development, the proposed module supports various different compilers. All of them are free, and user-modifiable:

- 1) **SCADA** executable: Visual Studio 2015 with C#.
- 2) **ATMEGA**: Arduino Compiler with Wiring language.
- 3) **NEXTION** LCD module: Nextion Editor

In order to make available the project design files, at circuit and schematic level, but also the corresponding software that has been developed, the GitHub sharing service has been selected, as one of the most common free servers available for such purposes. A snapshot of the software interface developed for this board is shown in Figure 5.

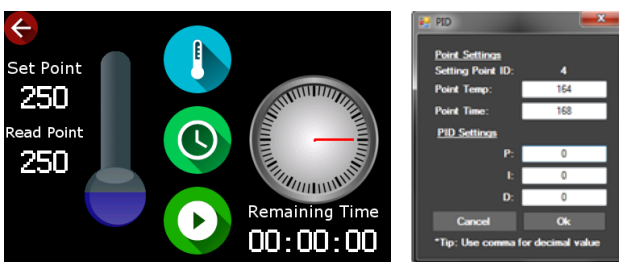


Figure 5. Nextion HMI Simple Oven Control HMI.

IV. SIMILAR OVENS

A number of reflow oven systems similar to this work is outlined below:

- **IP Holder Inc.** Very small board with open source C# program [12]
- **Zallus Learning Controller.** This is an inspiring implementation, especially due to the program design and communication method. It also employs a prediction control method [13].
- **ControLeo2.** Very simple oven controller with open source Arduino code which also has very nice learning algorithm. [14]
- **X-Toaster.** Very impressive implementation with a graphical HMI [15]
- **Reflowster.** Very simple on-off controller which doesn't require any external switch element. [16]
- **Hobbybotics Reflow Controller.** Very instructional in controlling algorithms. [17]

V. CONCLUSION

This work presents a custom microcontroller module with multiple inputs and outputs and four power relays. The design is customized for controlling a reflow oven but allows for expansion to systems with both heating and active cooling. The design is available in the open source domain, and the proposed method can be applied to other thermal control applications beyond the reflow oven use case presented here. Test results are not implement it because it is still under development. Final tests will be available for preview on GitHub repository among other useful files for porting it on a different control applications and different OS.

REFERENCES

- [1] Reflow Soldering https://en.wikipedia.org/wiki/Reflow_soldering
- [2] Reflow Oven https://en.wikipedia.org/wiki/Reflow_oven.
- [3] Kester Reflow Profiles <http://www.kester.com/>
- [4] Reflow Soldering Processes and Troubleshooting by Ning-Cheng Lee.
- [5] LPKF <http://www.lpkf.com/>
- [6] BUNGARD <http://www.bungard.de/index.php/en/>
- [7] ATMEGA 2560 <http://www.atmel.com/devices/atmega2560.aspx>
- [8] MAX31855 <https://www.maximintegrated.com/en/products/analog/sensors-and-sensor-interface/MAX31855.html>
- [9] Arduino <https://www.arduino.cc/>
- [10] FT232 <http://www.ftdichip.com/Products/ICs/FT232R.htm>
- [11] NEXTION <https://nextion.ithead.cc/>
- [12] IP Holder Inc. <http://reflowcontroller.com/>
- [13] Zallus Learning Controller <http://www.zallus.com/controller/>
- [14] ControLeo2 <http://www.whizoo.com/>
- [15] X-Toaster <https://www.tindie.com/products/BreakTech/x-toaster--toaster-oven-reflow-controller-kit/>
- [16] Reflowster <http://reflowster.com/>
- [17] Hobbybotics Reflow Controller <https://hobbybotics.com/projects/hobbybotics-reflow-controller->

Smart Home Automation using Arduino and Android

Antonios Sylari, Konstantinos Stamatiou-Kalaitzakis, Konstantinos Kamoutsis, Evaggelos V. Hatzikos

Department of Automation Engineering, ATEI Thessaloniki

Abstract—This paper presents the design and implementation of a remotely controlled Smart Home model that aims for the resident's comfort and security. The system combines sensors and appliances activators to respectively get information from and control the house environment. As a central controller, we used an Arduino microcontroller that communicates with an Android mobile application through a web server. Among its advantages, an important one is the possibility to control and monitor the system with low cost. Another one is its flexibility since its features can vary upon the resident's demands.

Index Terms—Smart Home, Android device, Smartphone, Home Automation, Arduino

I. INTRODUCTION

SMART Home is the integration of technology and services through home networking for a better quality of living; it is a house that involves advanced automatic systems such as lighting, heating, and security. Smart home can provide remote control and monitor through a smartphone or a web site for various appliances.

The Smart Home Model presented in this paper consisted of various subsystems to control and monitor the home with an Android application. The first one refers to the security system with a PIR sensor, smoke sensor and limit switches. The second subsystem is about the control of lighting and electrical devices. The third includes a temperature sensor to open and close shutters to save energy. Finally, there are two scenarios to protect the home and also to minimize energy consumption. The main computer that controls and supervises the whole system is an Arduino Mega2560. We developed a web server through which our Android application can monitor and control the system.

II. CONNECTIVITY

To enable connectivity on the microcontroller, an Ethernet shield is used. This provides connectivity via the serial I/O pins on the Arduino. The Android based mobile application communicates with the microcontroller via the web server which allows the user to have internet access and control of the home.

A. Arduino

Arduino is an open-source design platform and easy-to-use hardware and software to create electronic projects. The microcontroller board that is used on this project is the Arduino Mega 2560, which is based on the ATmega2560. It has 54 digital input and output pins, 14 of which can produce PWM outputs and 16 analog inputs. It can be powered from a computer through a USB connection, a 9V battery or an AC-DC adapter.

TABLE I
ARDUINO MEGA 2560 SPECIFICATIONS

Microcontroller	ATmega2560
Operating Voltage	5V
Input Voltage	6-20V
Digital I/O Pins	54 (15 provide PWM output)
Analog Input Pins	16
DC Current per I/O Pin	20 mA
DC Current for 3.3V Pin	50 mA
Flash Memory	256 KB (8 KB used by bootloader)
Clock Speed	16 MHz

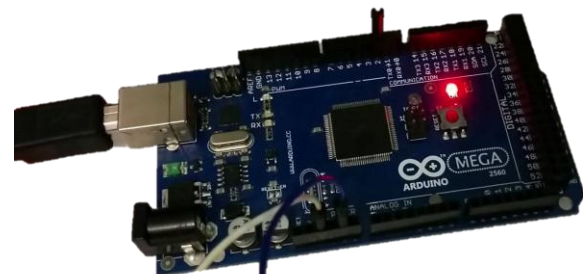


Fig. 1. Image of Arduino Mega 2560

B. Ethernet Shield

The Arduino Ethernet Shield allows an Arduino Board to connect to the internet. An Arduino Ethernet Shield V1 is used for this Smart Home Model which is based on the Wiznet W5100 Ethernet chip that provides a network (IP) stack capable of both TCP and UDP. The Ethernet Shield connects on an Arduino Board via long wire-wrap headers extending through the Shield which allows another shield to connect on it. Arduino engages 4 digital pins (10, 11, 12, and 13) for the internet communication which cannot be used as input or output pins. The Ethernet Shield has a standard RJ-45 connection, with an integrated line transformer and Power over Ethernet enabled. There is also a micro-SD card slot to store files for serving over the network. [8]



Fig. 2. Image of Arduino Ethernet Shield [8]

Editorial contents of the arduino, such as texts and photos, are released as Creative Commons Attribution ShareAlike 3.0

C. Android application

The android application was designed using the Google App-Inventor Integrated Development Environment (IDE). The application contains the web server's IP address, which interfaces with the micro-controller and allows the android smart phone to communicate with the microcontroller effectively and efficiently. The android application allows the user to control devices and monitor conditions in the home using internet connection.

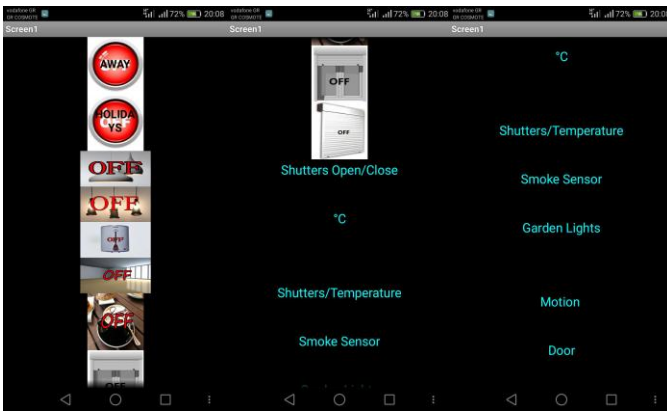


Fig. 3. Image of Android application

III. APPLICATIONS

The developed applications of Smart Home and security system are the following:

- Smoke sensor detects gas leaks or fire, enables the alarm and sends a notification to the application.
- PIR sensor detects movement in the place, enables the alarm and sends a notification to the application.
- Temperature sensor shows home's temperature on the application. The shutters open or close automatically depending on this temperature.
- Garden lights. A photoresistor turns on the garden lights when the sun goes down and turns off the lights when the sun rises.
- Limit switch installed on the door. The alarm is activated as soon as the door opens and sends a notification to the application.
- Soft buttons on the android applications are used to turn on and off lights, heater, coffee machine and shutters.

The most important applications are two scenarios, the AWAY scenario and the HOLIDAYS scenario. AWAY scenario is enabled from the application when the owner leaves the house for a short period of time during the day and disables all the electrical devices and lights that may be left on. HOLIDAYS scenario is applied when the owner is away from home for more than a day and for certain time switches on devices such as lights for security.

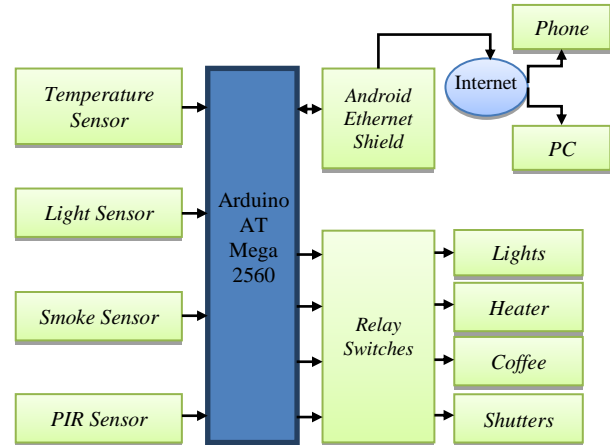


Fig. 4. Block Diagram of the Home Automation

IV. ACKNOWLEDGEMENT

We would like to thank our supervisor Dr. E. Hatzikos for his cooperation and support throughout the various stages of project development. This project is part of the research programme developed between the Department of Automation Engineering, ATEI Thessaloniki and Kafkas Company for Home Automation.

REFERENCES

- [1] Nathan David, Abafor Chima, Aronu Ugochukwu, Edoga Obinna, "Design of a Home Automation System Using Arduino", *IJSER*, vol. 6, Issue 6, pp 795-801, June 2015
- [2] Al-Qutayri, M.A., Jeedella, J.S.: Integrated Wireless Technologies for Smart Homes Applications. In Smart Home Systems, M. A. Al-Qutayri, Ed., ed: InTech (2010)
- [3] Vendela Redriksson, "What is a Smart Home or Building", (2011) April, Available at: <http://searchciomidmarket.techtarget.com/definition/smart-home-or-building>, Accessed: December 2016.
- [4] Molly Edmonds, "How Smart Homes Work - Setting Up a Smart Home", (2011), Available at: <http://home.howstuffworks.com/smart-home.htm>, Accessed: December 2016
- [5] Rosslin John Robles and Tai-hoon Kim, Applications, Systems and Methods in Smart Home Technology: A Review, *International Journal of Advanced Science and Technology*, Vol. 15, (2010) February, pp. 37-48.
- [6] P Pavan Kumar, G Tirumala Vasu, "Home Automation & Security System Using Arduino Android ADK", *IJETER*, vol. 3, no.6, pp 190-194, 2015
- [7] Mohamed Abd El-Latif Mowad, Ahmed Fathy, Ahmed Hafez, "Smart Home Automated Control System Using Android Application and Microcontroller", *IJSER*, vol. 5, Issue 5, pp 935-939, 2014
- [8] <https://www.arduino.cc>

Recent advancements in dynamic thermoelectric energy harvesting

M E Kiziroglou^{1,2,3}, P Goodrich², Th Becker⁴, S W Wright³,
E M Yeatman³, J W Evans² and P K Wright²

¹ATEI Thessaloniki, Greece

²University of California at Berkeley, CA, USA

³Imperial College London, U.K.

⁴Airbus Group Innovations, Germany

Energy harvesting is a technology that allows the exploitation of environmental energy to power local microsystems. It provides energy autonomy, lifting the burden of a wired connection to the power grid or the maintenance overhead of using replaceable or rechargeable batteries. Due to its highly novel nature and the extraordinary importance of the applications that energy harvesting is promising to enable, the establishment and recognition of performance boundaries and applicability limitations is critical to a correct interpretation. These performance boundaries have been clearly established and reconfirmed by various studies, showing great promise for self-powered wireless sensing nodes and actuating microsystems [1]. Applicability depends mainly on the environmental conditions, size and power requirements, and very importantly on the sensing scenario, which determines the necessary schedule of required power delivery. The evolution of dynamic thermoelectric energy harvesting, the transformation of temperature fluctuation into a local spatial temperature difference using a phase changing thermal mass, and heat flow exploitation by a thermoelectric generator, is a characteristic example that reveals the set of requirements that need to be met in order to develop a self-powered wireless sensor system. For this reason, in this presentation recent advancements in the field of dynamic thermoelectric energy harvesting are reviewed. This review includes analytical calculations, numerical modelling, modelling extensions to account for effects such as super-cooling and inhomogeneous phase change, device fabrication and characterisation, and integration into complete wireless sensor networks. The main potential application of this technology is powering wireless sensors located at environments involving temperature fluctuation.

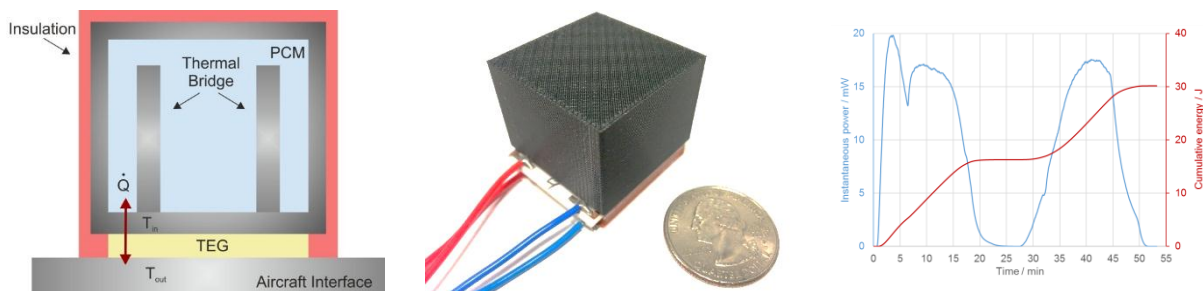


Figure 1. (left) Schematic illustration of the dynamic thermoelectric energy harvesting concept. (middle) Photograph of a device prototype [2], (right) Measured power output from a temperature cycle between +20 °C and -20 °C.

References

- [1] P. D. Mitcheson, E. M. Yeatman, G. K. Rao, A. S. Holmes, and T. C. Green, 'Energy harvesting from human and machine motion for wireless electronic devices', *Proceedings of the IEEE*, vol. 96, pp. 457–1486, 2008.
- [2] M. E. Kiziroglou, Th Becker, S W Wright, E M Yeatman, J W Evans and P K Wright, *Thermoelectric Generator Design in Dynamic Thermoelectric Energy Harvesting*, PowerMEMS, Paris, France, Dec. 6-9, 2016.